A DISTURBANCE-OBSERVER-BASED CONTROLLER FOR LLRF SYSTEMS

F. QIU#, D. ARAKAWA, Y. HONDA, H. KATAGIRI, T. MATSUMOTO, S. MICHIZONO, T. MIURA, T. OBINA, KEK, Tsukuba, Ibaraki 305-0801, Japan
S. B.WIBOWO, SOKENDAI (the Graduate University for Advanced Studies), Tsukuba, Japan

Abstract

Digital low-level radio frequency (LLRFs) systems have been developed and evaluated in the compact energy recovery linac (cERL) at KEK. The required RF stabilities are 0.1% rms in amplitude and 0.1° rms in phase. These requirements are satisfied by applying digital LLRF systems. To further enhance the control system and make it robust to disturbances such as large power supply (PS) ripples and high-intensity beams, we have designed and developed a disturbance observer (DOB)-based control method. This method utilizes the RF system model, which can be acquired using modern system identification methods. Experiments show that the proposed DOB-based controller is more effective in the presence of high disturbances compared with the conventional proportional and integral (PI) controller. In this paper, we present the preliminary results based on the experiments with DOB-based controller.

INTRODUCTION

At KEK, a 3 GeV energy recover linac (ERL) light source is proposed. For the demonstration, a compact ERL (cERL) was constructed as a prototype machine for the 3-GeV ERL project [1,2]. The cERL, which is a 1.3 GHz superconducting (SC) project, consists of an injector part and a recirculating loop part. Three two-cell cavities, called Inj. 1, Inj. 2, and Inj. 3, were installed in the injector, and two main nine-cell cavities were installed in the recirculating loop. To fulfill the required beam quality, the RF field fluctuations should be maintained at less than 0.1% (in amplitude) and 0.1° (in phase) in the cERL. Field programmable gate array (FPGA)-based digital low-level ratio frequency (LLRF) systems were developed to implement the RF field control [3].

In the LLRF systems of the cERL, disturbance signals such as 50-Hz microphonics and 300 Hz high-voltage power supply (HVPS) ripples will severely limit the performance of the LLRF systems [3]. Furthermore, during beam commissioning, the beam loading can be seen as another disturbance. In principle, these disturbance signals can be rejected or suppressed by applying high proportional and integral (PI) gains in the feedback (FB) control; however, the PI gains are limited by the loop delay. In the cERL, during the beam commissioning, we found that the PI gain is not sufficient in the presence of large disturbances. In view of this situation, we present a disturbance observer (DOB)-based approach that aims to control an LLRF system subject to large disturbances [4-5].

In this paper, we first introduce the LLRF system in the cERL, and then describe the principle, design, and implementation of this DOB-based approach. Finally, preliminary results are used to compare the proposed DOB control and the previous PI control in the cERL beam commissioning.

LLRF SYSTEM

A simplified block diagram of the cERL LLRF system is shown in Fig. 1. The 1.3-GHz cavity probe signal is down-converted to a 10-MHz intermediate frequency (IF) signal. The IF signals are sampled at 80 MHz by 16-bit ADCs and then fed into the FPGA. The baseband and quadrature (I/Q) components are extracted from the IF signal with a non-IQ method. In the next stage, the I/Q signals are compared with their set values, and the errors are calculated. The errors are regulated with a PI controller and then added with a feedforward (FF) table. Finally, the combined signal is fed into the I/Q modulator via the 16-bit DACs to regenerate the 1.3-GHz RF signal. This regulated RF signal will be used to drive the high-power source, which drives the cavities [6,7].

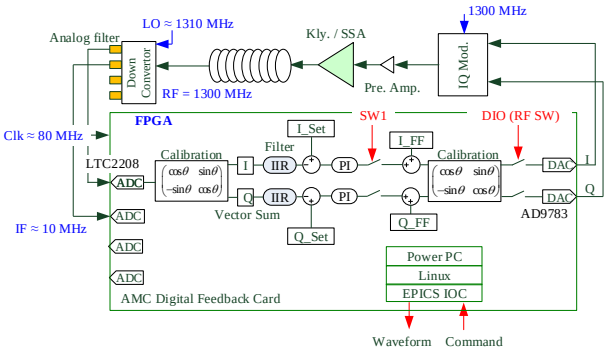

Figure 1: Schematic of the LLRF system in the cERL.

DOB CONTROL

The basic idea of DOB control is shown in Fig. 2(a) [4-5]. Here, $G_p(s)$ and $G_n(s)$ represent the transfer function of the actual plant (e.g., cavities and RF devices) and the nominal mathematical model. Signals d and d_e represent the real disturbance and the disturbance estimate, respectively. Signal FF represents the FF table output.

From Fig. 2(a), it is clear that the disturbance estimate d_e can be expressed by

#qiufeng@post.kek.jp

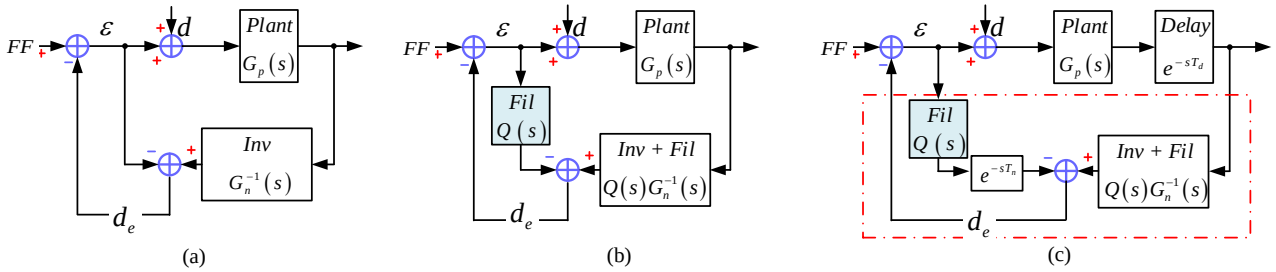

Figure 2: Evolution of DOB control. From left to right: (a) the basic structure of DOB control, (b) DOB control with Q filter, (c) DOB control with Q filter and delay compensation unit.

$$d_e = (\varepsilon + d)G_p(s)G_n^{-1}(s) - \varepsilon. \quad (1)$$

If the the inverse nominal model $G_n^{-1}(s)$ (which can be acquired by applying system identification [6,7]) is sufficiently accurate, the signal d_e is a good estimate of the disturbance signal d; i.e., the disturbance signal can be observed and then reproduced if we know the system models very well. Therefore, after removing the signal d_e from the FF table (see Fig. 1), the disturbances are compensated.

In practice, a Q filter is usually required as shown in Fig. 2(b). The main function of the Q filter is to make the combined transfer function $Q(s)G_n^{-1}(s)$ a casual system that is physically realizable (the $G_n^{-1}(s)$ is usually anti-casual in practice). The selection of the Q filter is one of the key issues in the DOB controller design. References [4-5] describe good Q filter candidates. In the cERL LLRF system, our selection is a second-order filter as given in

$$Q(s) = \frac{1}{(\tau s + 1)^2}. \quad (2)$$

The time delay is another issue that needs to be considered. Suppose parameter T_n is an estimate of the actual time delay T_d, then as shown in Fig. 2(c), an extra delay model is added in the DOB controller to compensate for the time delay of the system. From Fig. 2(c), it is clear that we can update the disturbance estimate d_e as

$$d_e = (\varepsilon + d)G_p(s)e^{-sT_d}G_n^{-1}(s)Q(s) - \varepsilon Q(s)e^{-sT_n}. \quad (3)$$

Therefore, on the basis of (3), if the system model is sufficiently accurate, and the filter Q(s) outputs 0 dB in the frequency band of interest, which covers the classic disturbance frequencies (e.g., DC to 1 kHz), the signal d_e is a good representation of the actual disturbance d.

ANALYTICAL STUDY

The integration of the DOB controller and the previous PI feedback system is shown in Fig. 3. The DOB-based controller is indicated by the red block. The switch SW2 in the figure control the enable/disable operation of the DOB controller.

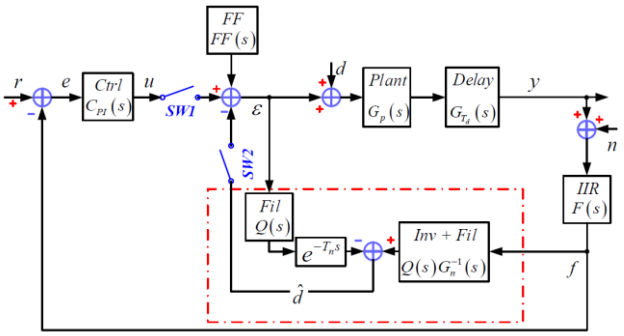

Figure 3: Integration of DOB control and PI control. The presented DOB controller is indicated by the red block.

The closed-loop Bode plots with and without DOB control are shown in Fig. 4. Here, we select the two most critical transfer functions in the system to analyze, which are the disturbance d and the noise n, to the cavity pick-up y ($d \rightarrow y$ and $n \rightarrow y$). The location of each signal is given in Fig. 3. The Q filter in the DOB controller is specified according to (2), with a 5-kHz cutoff bandwidth.

Figure 4(a) indicates that the proposed DOB control shows great superiority in disturbance rejection compared with the PI control, especially for the frequency range from DC to 10 kHz. This is also the most attractive advantage of the DOB control. Figure 4(b) shows that there is no obvious difference in noise suppression for these two approaches.

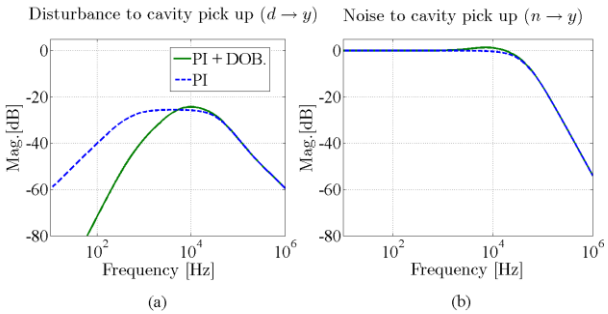

Figure 4: Closed-loop system response comparison of PI control and "PI+DOB" control. From left to right: (a) Disturbance to cavity pick-up ($d \rightarrow y$); (b) Noise to cavity pick-up ($n \rightarrow y$).

EXPERIMENT ON CERL BEAM COMMSIIIONING

We have developed this DOB-based controller in an FPGA and demonstrated it in the digital LLRF system of the injector. The main parameters of the RF system and cavities are listed in Table 1. In the HVPS of the 300 kW klystron, which drives Inj. 2 and Inj. 3, the 300 Hz component is one of the main disturbances. On the other hand, in the presence of the high-intensity beam current under burst mode operation, beam loading is another important disturbance. We will present each of these two cases separately.

Table 1: LLRF and Cavity Parameters of the Injector

Cavity	**Inj. 1**	**Inj.2**	**Inj.3**
Cavity volt. (V_c)	0.7 MV	0.65 MV	0.65 MV
Beam phase (φ_b)	0°	0°	0°
Ctrl method	Individual	Vector-sum control	
Power source	20 kW kly.	300 kW kly.	
Loaded Q (Q_L)	1.2×10^6	5.7×10^5	4.8×10^5

HVPS Ripple Rejection

Figure 5 compares the PI control (blue) and the PI+DOB control (red) for the LLRF systems on Inj. 2 and Inj. 3. It should be mentioned that the PI gains, which are optimized with a gain-scanning experiment [7], are identical in both the control approaches. The second-order IIR filter, which is the discrete form of (2), with 5 kHz bandwidth, is selected as the Q filter. Fast Fourier transform (FFT) results demonstrate that the 300-Hz HVPS ripples are clearly rejected after applying the DOB control. The amplitude and phase stability improve from 0.03% and 0.029° to 0.026% and 0.018°, respectively.

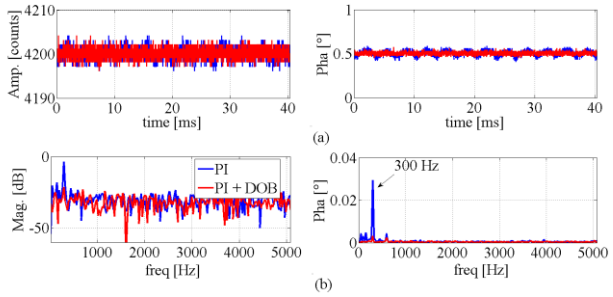

Figure 5: FB control (blue) vs. FB+DOB control (red). RF field performance in amplitude and phase is plotted as well as their FFT analysis. From top to bottom: (a) waveform, (b) FFT.

Beam-loading Compensation

During the cERL beam commissioning, a 1 mA beam current is operated for approximately 1 ms in burst mode. The beam loading here can be considered as a disturbance. The PI control is not sufficient to compensate for the beam-loading effect in the beam commissioning; therefore, we apply the proposed DOB control to compensate for the beam-loading effects.

Figure 6 shows the results of the beam-loading compensation experiment under 1.6 ms, 800 μA (peak value), and a 5 Hz beam pulse. Results of the PI control (blue) and the PI+DOB control (red) on both Inj.1 and Inj. 2&3 (vector sum) are compared in Fig. 6. It should be mentioned that the Q filter here is identical to the one employed in the HVPS rejection experiment. The improvement in the DOB control is evident in both cavities, as shown in Fig. 6. The beam loading is compensated for successfully in the presence of the DOB control.

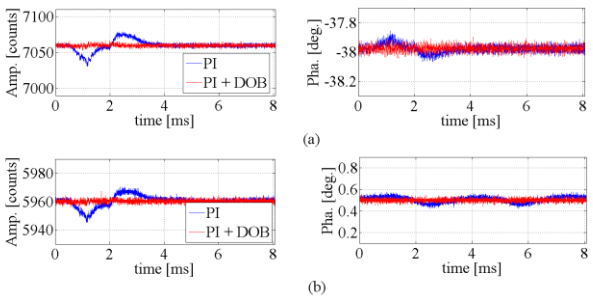

Figure 6: Measured RF field for the amplitude (left) and the phase (right) in the cavities of the injector in the presence of 800-μA beam loading. Red and blue waveforms in each subplot represent the PI control and the PI+DOB control, respectively. From top to bottom: (a) Inj. 1, (b) Inj. 2&3.

SUMMARY

During the beam cERL commissioning, the LLRF system performance is limited by several types of disturbances, mainly the 300-Hz HVPS ripples and beam loading. The previous PI control is not sufficient to reject these disturbances. In this study, a DOB-based control approach for disturbance rejection was developed. Both the 300 Hz HVPS ripples and beam loading are successfully compensated for with this DOB-based approach. In this paper, we presented the idea and the preliminary results of this approach.

REFERENCES

[1] N. Nakamura et al., "Present status of the compact ERL at KEK," Proc. IPAC2014, Dresden, Germany (2014).

[2] S. Sakanaka et al., "Construction and commissioning of compact-ERL Injector at KEK," Proc. ERL2013, Novosibirsk, Russia (2013).

[3] T. Miura, “Performance of RF systems for compact ERL injector at KEK,” Proc. ERL 2013, Novosibirsk, Russia (2013).
[4] C.J. Kempf et al., “Disturbance observer and feedforward design for a high-speed direct-drive positioning table,” IEEE Trans. Contr. Syst. Technol., 7(5), Sept. (1999).
[5] T. Umeno and Y. Hori, “Robust speed control of dc servomotors using modern two degrees-of-freedom controller design,” IEEE Trans. Ind. Electron., vol. 38, no. 5, pp. 363–368 (1991).
[6] F. Qiu et al., “Digital filters used for digital feedback system at cERL,” LINAC14, Geneva, Switzerland (2014).
[7] F. Qiu et al., “Evaluation of the superconducting LLRF system at cERL in KEK,” IPAC13, Shanghai (2013).